

## Analysis and characterization of 20 ppi open cell aluminum foam under mechanical loading

S. Hussain\*, A. Shakoor<sup>1</sup>, T. Yasmin

Faculty of Mechanical Engineering, University of Engineering and Technology Peshawar, 25000, Pakistan.  
Phone: +92-91- 9222217, Fax.: +92-91- 9216663

**ABSTRACT** – In this research the analysis and characterization of open cell aluminium foam with 20 pores per inch (ppi) of Alporas rout under mechanical loading is presented in order to provide a basic understanding with respect to pore size per unit length for the right selection in various engineering applications. For this purpose, three point bending test, tensile test, compression test, vickers hardness test and charpy impact test were performed to seek out the respective properties of each test. All samples and test procedure were performed as per ASTM standards. The scanning electron microscopy (SEM) will be performed of the fractured surfaces of the specimens to investigate the failure mode. The SEM photograph shows that; some internal defects were found such as the tiny cracks some irregular shape holes in the cell wall which have been created during foaming process. The shredded cell wall is looked over which was ductile in nature and have occurred during flexural, tensile and charpy impact test. In compression; all pores are collapsed in plateau region, and some crumples and brittle tiny cracks are detected in densifications stage. Dislocation band also detected on the walls and struts of the effected sample of tensile and charpy impact test.

### ARTICLE HISTORY

Received: 22<sup>nd</sup> May 2022

Revised: 16<sup>th</sup> Aug. 2022

Accepted: 09<sup>th</sup> Sept. 2022

### KEYWORDS

*Open cell aluminum foam*

*Characterization*

*Mechanical loading*

*Scanning electron microscopy*

*Alporas rout*

*Pores per inch (ppi)*

## INTRODUCTION

Metallic foams are composed of macro-cells which are characterized by solid-state strong material encompassed by 3D organization of voids. Metal foam is a new type of material having interesting and attractive mechanical and physical indications. Because of their cellular, strong and porous construction it has light weight, good strength and high energy engrossment capability owing to which its agreeable choice for the practical life application in different area. Aluminum foam is a young class of metallic foam which have enclosed of inviting indications such as light weight, good strength, excellent energy engrossment and heat diffusion and transfer features. Due to these all core performance the aluminum foam is a best candidate for the space industry, automobile sectors, locomotive, packing and other different zones [1-6].

As per construction of cells and voids aluminum foam has broken into two major family open cell and closed cell aluminum foam. Open cell aluminum foam composed of only ligaments and edges that there are an open space exist between two adjacent cells, which is created by Alporas rout, spaceholder and foam casting method while closed cell aluminum foam comprised of solid-state that each cells and pores is closed off from adjacent cells which is created by melt foaming; powder metallurgy and gas injection process.

The utilizations and properties of aluminum foam relies on their fundamental qualities, for example cells and pores construction, size and dispersion as well as highly effected on manufacturing method [7]. The manufacturing process of aluminum foam is very complicated because every manufacturer creates different kind of foams due to the less research encourage. The construction of cells and voids of aluminum foam are organized in such a way that they resist an extensive deformation under mechanical loading and engulf magnificent energy before rupture of cell and voids geometry [8]. A lot of investigations have focused on the behavior of aluminum foam to show that they have engulfed significant energy during compression and impact loading [9-15].

Aluminum foam exhibits three different zones (I-elastic, II-plateau and II-densification) of deformation during compression work in stress-strain graph. The first zone is elastic deformation in which cells of the foam deformed elastically and retain its original shape after removal of load. The second zone is called plateau territory which very important and responsible for engrossment of energy during compression load, in this territory the cells of foam shrink plastically and does not go back to past era. The plateau zone is originated by the creations and colonization of the cell-bands during deformation. In third zone the combination and compaction of cell-bands occurred which is called densification [16].

Shunmugasamy [17] conducted the compression test on cast and rolled foam with the strain rang limit of  $10^{-4}$  to  $10^3$  per second and discovered that the foam which was rolled exhibit higher plateau zone than unrolled. The value of strain hardening is also show higher than unrolled.

S.Y. Yang [18] performed and examined the three point bending attitude of aluminum foam having smooth face with 79.3% to 85% porosity manufactured via melt foaming process and realized that failing of sample occurred in three phases the first is elastic deformation, second is skin failure and the third is foam failure.

The aluminum with closed cell structure by using slow-rate compression and projectile collision/stroke with different speed ranging from 9.2 m/s to 36.5 m/s of projectile with the help of gun operated by air pressure. He discovered that the plateau-level of stress is increased by augment of density and also found anisotropic manner. During impact experiment he found that plateau-stress is insufficient to measure the projectile movement/motion during impact-load on aluminum foam [14].

The aluminum foam manufactured by using calcium carbonate ( $\text{CaCO}_3$ ) and magnesium carbonate ( $\text{MgCO}_3$ ) as blowing agent instead of titanium, has lesser density and low price which have excellent mechanical properties and can be suitable for automotive sectors. The titanium is very expensive which is used for aerospace anatomy [19].

The more extensive application scope of aluminum foam, the working environment and deformation mechanism of cells is more complex when often subjected to mechanical loading during their service [20]. Therefore the fundamental understanding and behavior of Aluminum foam is required. In other side foaming process is very complex because every manufacturer creates different type of foam owing to insufficient research encouraged of researchers to find different type of properties of Aluminum foam in different condition.

Being a novel material open cell aluminum foam can be manufactured by different routes (Alporas rout ,investment casting rout, space holder rout, chemical decomposition method) and each manufacturing rout highly effected the mechanical, thermal and physical properties of the same foam and due to which each manufacturer find different types of properties in different conditions.

The cell size of aluminum foam is also highly influenced the mechanical performance during their service, and there is no proper data available and has no one focused on these aspect, therefore it necessary to study the basic understanding and comparisons of aluminum foam with respect to the cell size per unit length.

This research is intent to contribute the above causes and focused on the analysis and characterization of open cell aluminum foam with 20 pores per inch (ppi) manufactured through Alporas rout under mechanical loading. A series of tests; three point bending test, tensile test, compression test, hardness test and charpy impact were conducted to find out their respective properties in each test. The scanning electron microscopy (SEM) will performed of the fractured surfaces of the tested samples to examine the failure nature of the aluminum foam. After the experimental tests the result and discussions will be made on basis of graphs, tables and images. The research result of this investigation can be used as guidance for the engineering design and application of the Aluminum foam in mechanical loading.

## Applications of Metallic Foam

The patent technology of sosnick had given earliest indication of metallic foam preparation. The first aluminum foam was invented by Borksten Research Laboratory Inc. in 1956 [21, 22]. After these inventions Japan had step forwarded and focused in metallic foam research material in 1987 [23]. In comparison with traditional materials aluminum foam have greater advantages of light weight, good strength, excellent energy engrossment and heat diffusion and transfer features, due to all these core performance the aluminum foam is one of the best candidate in advance technology material and research in the entire world.

Automobile sectors, railway and aerospace industries meet all requirements, that is found in aluminum foam such as light weight, energy engrossment and stiffness for safety and low fuel consumption because with light it has ability to engross high energy (in plateau regime) during impact and crash. Load sustaining and conveying performance in the structure, the closed cell aluminum foam exhibits outstanding outcome when it packed in between two plates (sandwich panel). Closed cell aluminum foam is a nice and successful choice for sounds and mechanical vibrations engrossment for mechanical system where vibration needed to minimize. Aluminum foam has also a great potential in application of heat dissipation and conduction devices because of their excellent acoustic features and thermal control [23]. For safe packaging and protection, aluminum foam is good choice for packaging industries because they have ability of longer, flat load bending features [14]. Porous metals have ability of exhibiting large deformation strain with constant stress in plateau zone features, making them a premier option for high impact and blast energy engrossment devices [16]. Metallic foam reveal a pronounce performance in corrosion resistance, non-inflammability and stiffness, so they can be used in orthopedic filed for the replacement of crashed bones [24]. Shortly metallic foam are widely using in entire world in numerous engineering applications due to their interesting core performance and features.

## EXPERIMENTAL WORK

### Material and Experimental Procedure

The open-cell aluminum foam with 20 pores size per inch (ppi) are used in this study, supplied by China Beihei composite company manufactured via Alporas rout. In this manufacturing rout, aluminum billets are melted at 700 °C and fine calcium particles were added in molten aluminum and agitate for 8 to 10 minutes at 700 revolutions per minutes (rpm) of stirring machine. The viscosity of melted aluminum is amplify and reached at desired value because of oxides and intermetallic formation owing to addition of calcium. Then 1-2 wt. % of  $\text{TiH}_2$  is added and agitates for 1000 rpm for 1.5 to 3 minutes, meanwhile it decompose inside the melt owing to effect of heat and release hydrogen gas and released gas gets trapped in the melt which make the melted medium pours and finally it gets gently transformed into solid pours structure after instantaneous solidification. The relative density noted up to 0.25, calculated after slabs cutting from

base/block material. Cell sizes and cell wall thickness observed round about 2 to 10 mm and 100 to 300  $\mu\text{m}$  respectively [14].

### Three Point Bending Test

For this setup “American Society for Testing and Materials” ASTM- E290-14 and D7972-14 are followed for testing techniques and preparation of samples respectively. Three samples with same size were cut from the slab and kept the dimensions  $L=120\text{mm}$   $B=30\text{mm}$  and  $T=15\text{mm}$ . An electro-mechanical universal testing machine (Testometric, Model-M500-30AT) were used provided by “US-Pakistan Center for Advance Studies in Energy” UET Peshawar. In this machine sample are placed on two roller supports and apply load at the center of the sample as shown in Figure 1. The machine was set on 1mm/min mandrel loading rate at the  $90^\circ$  to sample. The experiment was accomplished at normal room temperature. The span of the beam/sample between the two supports was kept 65 mm as computed by given Eq. (1).

$$C = 2r + 3t \pm t/2 \quad (1)$$

Where,  $C$  is the span of the sample between support,  $r$  is radius of mandrel and roller support and  $t$  is thickness of sample. The radius of the end of the mandrel and roller supports of the machine were used 10 mm. For each tested samples a graph between force ‘ $F$ ’ (N) of mandrel and deflection ‘ $\delta$ ’ (mm) of beam/sample were generated. The failure fashion and location failure of each specimen were observed and recognized from  $F-\delta$  graph. The peak value of deformation force (break force) at which failure occurred was also identified in the graph.

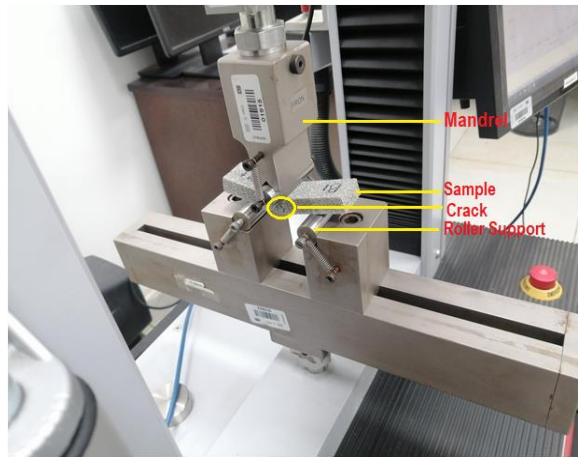


**Figure 1.** Three point bending test machine apply load with 1 mm/min on sample until fracture

### Tensile Test

In this arrangement tensile test were performed by adopting universal testing machine (Testometric) provided by Centralized Resource Laboratory (CRL), University of Peshawar. The dog-bone shaped samples were fabricated with same size and dimensions were  $L=71\text{mm}$ ,  $B=15\text{mm}$  and  $W=8\text{mm}$  as per standard ASTM E8-15A for better and satisfactory result. In this setup the shoulders of the dog-bone shaped sample are securely tight at two opposite grip of the machine. The machine elongates/pulls the sample with a constant strain rate of 1mm/minute up to breakup point as shown in Figure 2. During experiment strain/change in length of the sample were measured with the help of sensor attached with crosshead of universal testing machine (UTM). At the same time maximum acting load on sample noted for the construction of stress strain curves. Each sample was tested three times and graph was drawn from date (force/load and strain) gathered during experiment.

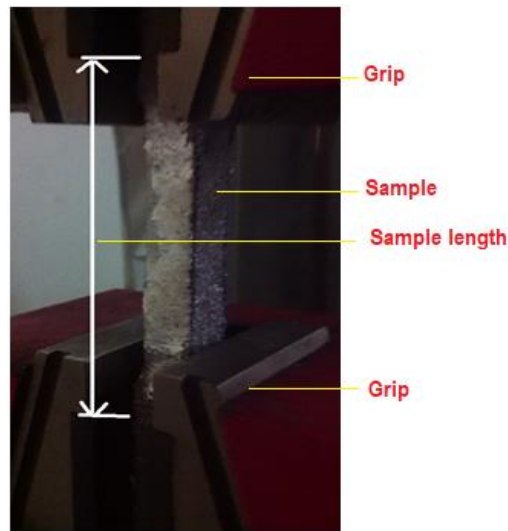


**Figure 2.** Universal testing machine elongate the sample with constant strain rate of 1 mm/min until fracture

### Compression Test

One of the aim of this investigation is to accomplish a compression test by using universal testing machine (Testometric) provided by physics Department University of Peshawar as shown in figure 3.15. For this setup cube shaped samples were manufactured with same size and dimensions were  $L=34.1$  mm,  $H=34.1$  mm and  $W=15$  mm according to standard ASTM C-365M. Each sample was repeated three times for better and satisfactory result. In this experiment sample are placed securely on 'sample holder' of the lower ram of the machine and apply load by the downward movement of the upper ram on sample as shown in Figure 3. The machine was set on 1mm/min of upper ram movement/loading rat on sample. The experiment was accomplished at normal room temperature. During experiment, for every tested sample an information regarding load/force 'F' (N) of the upper ram and deflection 'δ' (mm) of sample until failure could be noted. The failure fashion and location of each specimen were observed and identified. The peak value of deformation force (failure force) at which failure occurred were also identified and noted for further discussion of aluminum foams on the basis of their porosity. The value of compressive strength/stress ( $\sigma$ ) and corresponding strain ( $\epsilon$ ) can be computed by using Eqs. (2) and (3) as given below. In given equations  $A_i$  represents initial area of sample expose to load,  $\Delta h$  is deformation in the direction of compressive load and  $h_i$  is initial height of sample.

$$\sigma = F / A_i \quad (2)$$

$$\epsilon = \Delta h / h_i \quad (3)$$

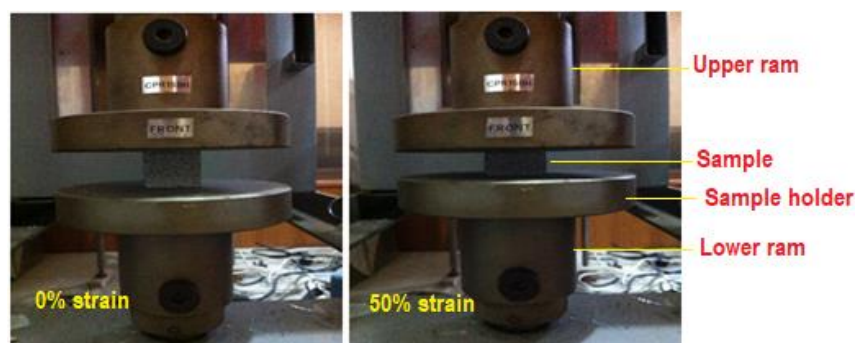


**Figure 3.** Machine apply constant loading rate of 1mm/min upon sample until fracture

### Hardness Test

For this setup "American Society for Testing and Materials" ASTM- E18-20 and E110-14 are followed for testing techniques and preparation of samples respectively. For samples preparation, it is highly suggested that the thickness of sample must beyond the 10-times of 'indentation depth' and there is no visible effect of the indentation on the back side of the sample after experiment. A digital universal hardness testing machine (Tinius-olsen, Model-H-002-0001) were used provided by "US-Pakistan Center for Advance Studies in Energy" UET Peshawar. In this hardness machine the required sample is placed on the anvil properly. Then the machine was programmed to apply 1 kilogram-force (1 kgf) on the sample surface perpendicularly for the duration of 10 seconds, which refer as dwelling time as shown in Figure 4.

Diamond pyramid shape having square base indenter was used for loading and depth of indentation. The machine calculates value of hardness on the base of 'indentation depth' in the surface of sample as shown in figure 3.8. Actually hardness machine used an Eq. (4)/formula programmed in their integrated circuit (IC) as mentioned below. Each sample was tested four times and find out the average value of each sample. The space between the center of two nearest indentation were kept 3 times the dia (d) of indentation as shown in Figure 5.

$$HV = F/d^2 \times 1.854 \quad (4)$$

Where, HV represents vickers hardness, F is apply load in kgf and d is the average of the diagonals diameters of the indentation.

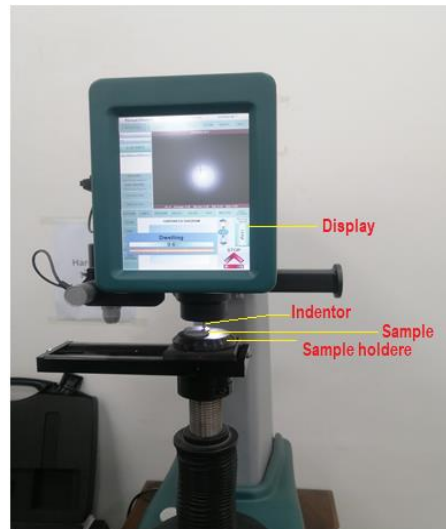


**Figure 4.** Sample is placed on specimen holder and indenter apply load on sample of 1 kgf for 10 second

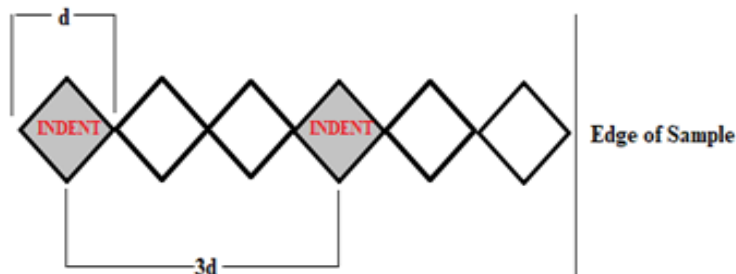


**Figure 5.** Schematic diagram of space between two nearest indentations

### Charpy Impact Test

A V-notched with 45 degree<sup>o</sup> samples were manufactured with same size and dimensions were L=45 mm, B=6 mm and W=6 mm according to standard ASTM E-23. This was accomplished by charpy impact test machine provided by University of Engineering and Technology, Peshawar. In this set up sample is securely and properly placed in sample holder of the machine. The hammer/pendulum of the machine was dropped from known height on the sample with 10 m/sec velocity as shown in Figure 6. The hammer strikes on the opposite side of the notch of the sample. After the strikes of hammer/pendulum with sample, the movement of the hammer arm decrease and this decrease will lead for the calculation of energy absorbed during experiment. The energy transfer to material can be found from difference between height of hammer before and after the fracture. Together with transfer of energy some amount of energy is dissipated, which can be computed from weight of pendulum and difference of pendulum height in each side (initial & final state) as by Eq. (5) given below. The experiment was accomplished at normal room temperature.

$$E = mg (h_i - h_f) \quad (5)$$

Where E is energy dissipated, m is mass of hammer of charpy impact test machine, g is gravitational force, h<sub>i</sub> is initial height and h<sub>f</sub> is final height of hammer.



**Figure 6.** Charpy impact test machine

### Scanning Electron Microscopy

This research is also aim to investigate to cell morphology and microstructure of aluminum foam of 20 ppi after experiments to seek the cell failure fashion and behavior of each tested sample. In Figure 7 the scanning electron microscope (JEOL, Model: JSM-IT-100, Made: Japan) provided by ‘National Centre of Excellence in Geology (NCEG), University of Peshawar. The sample could be taken for SEM from effected area of the tested sample. The sample size were made as per the requirement of the SEM specimen holder and the each samples of were coated with gold to make surface of the sample conductive. A smart coater machine is used for gold coating of sample surface as shown in Figure 8.



**Figure 7.** Scanning electron microscope setup



**Figure 8.** Specimen surface coater machine

## EXPERIMENTAL RESULTS

### Three Point Bending Test

Figure 9 shows force versus displacement curves of 20 ppi under three point bending test/flexural test of the three samples. The details parameters, properties and their average value of each tested sample were summarized in Table 1. The curve of 20ppi-1 exhibited the unique behavior in which load/force (N) reached to highest value of 454.2 N with minimal displacement of 1.554 mm and shown maximum 6.561 MPa bending strength as compared to other two samples of the same pore sizes. But it is important to note that, the curve of 20ppi-1 reached to highest value of force then goes down slightly and followed by dramatically fall down and reached to ground level. Suddenly and dramatically drop of curve of 20ppi-1 and 20ppi-2 is caused by the defected and imperfected as well as brittleness of cells and cell walls of the foam which may arose in during manufacturing process. The variations in curves of 20ppi-1, 20ppi-2 and 20ppi-3 may cause the orientations of the cell to the applied load is different in each sample. The bending policy of the all three sample of the 20 ppi occurred in three steps: (i)-step 'elastic deformation region' in this region the pores walls experienced deformation elastically and retain its original shape after removal of load, (ii)-step creation and appearance of micro cracks in pores/cell wall, in this stage the curve become slightly depressed and reached up to maximum value of load and cracks appears in all pores in jurisdiction of applied load when load reached up to peak value, (iii)-step is the failure stage, in this stage micro-cracks of each cells starts propagation and grow up and finally each crack of the each cells joints one another as a result of which a macro crack appears in outer surface of the sample center and sample becomes fails. The top point of the curves represents the bending failure force (N) of the foam. Furthermore, the curve behavior falls down gradually with decreasing load (N) in comparison to increasing displacement as shown by 20ppi-2. From the SEM image of the fractured surface of the tested samples as shown in Figure 10 the shredded cell wall of the two adjoining cell were looked-over and looking like ductile in nature, which was occurred during bending load test as represented by red circles. Moreover some patterned groves but not deeper, were noticed on the surface of the cell wall which may also tack active part in the creations of micro cracks during bending test, as shown in by yellow box. The irregularities of the cell shape were observed which may lead to poor performance in bending application.

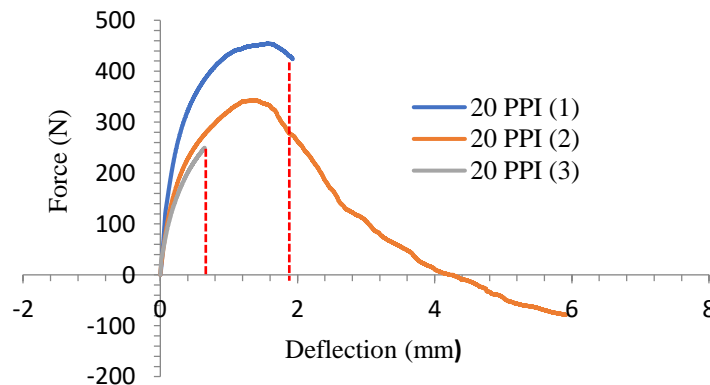


**Figure 9.** Force versus Deflection curves of the three samples of 20 ppi under flexural test

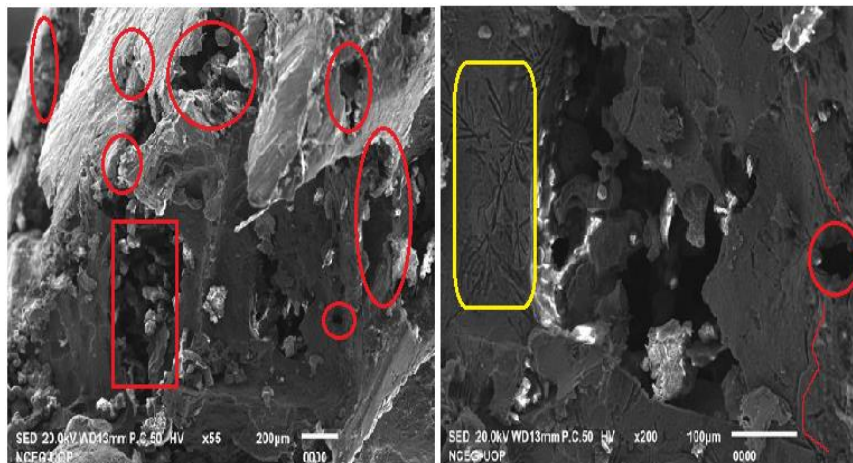


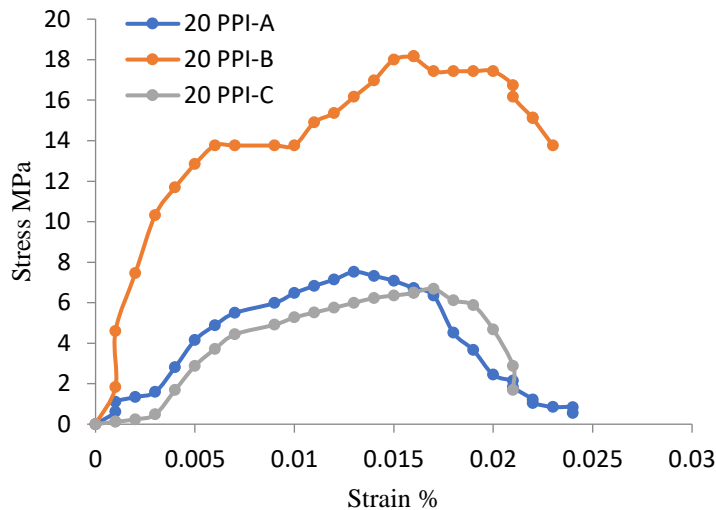
**Figure 10.** SEM micrograph of fracture surface of 20 pores per inch after flexural test

**Table 1.** Flexural properties of 20 ppi of open cell aluminum foam by Alporas rout

Samples	Sample Dimensions (LxWxT) mm <sup>3</sup>	Force at Peak (N)	Deformation at Peak (mm)	Deformation at Break (mm)	Bending Strength at Peak (MPa)	Bending Strength at Break (MPa)
20-A	120x30x15	454.2	1.554	1.931	6.561	-834.586
20-B	120x30x15	342.7	1.351	5.915	4.95	-1.138
20-C	120x30x15	176.3	0.444	1.241	2.547	0.994
Average	-	324.4	1.12	3.029	4.686	-

### Tensile Test

Figure 11 shows stress versus strain curves of 20 ppi under tensile test of the three samples of the same pores. The details parameters, properties and their average value of each tested sample were summarized in Table 2. The sample 20-B shows outlying properties in the graph. Its elastic strength is 1265.9 MPa is very higher and shown maximum 18 MPa ultimate tensile strength (UTS) as compared to other two specimens for same pore sizes. However the other two specimens show a strange behavior in the graph. The samples 20-A and 20-C specimens for 20 pores per inch are showing a flat curve after reaching their elastic limit. This shows increase in strain at expense of constant stress. This constant behaviour can be attributed to the elongation of already elastically elongated cell walls of metal foam. This behaviour is similar to plastic deformation flow region where stress cause a permanent increase in length of material without application of extra stress causing material to flow. This behaviour was not global phenomena because it is repeated again and again in the graph. Furthermore the uniformity in results can also be contributed to constant porosity i.e. constant pore volume throughout the solid and the orientations of cells subjected to the load in each sample. The uniformity of the cell makes material to behave as homogenous solid giving a uniform result. Figure 12 expresses the microstructure of fractured surface of specimens after the tensile test. Some randomly internal defects and flaw were found in the cell wall and matrix/struts of aluminum foam and these internal defects are the tinny cracks some irregular shape holes in the cell wall/membrane as represented by red circles. These defects may facilitate in failure of the aluminum foam and reduce the mechanical performance because more stress concentrate at defected zone and help to assist first crack generation and propagations during load. Furthermore the internal defects looked over more opened when it experience tensile axial load and first micro crack is create when stress reached to critical value in a plastic zone of the material. When first crack is initiated from the defected area during tensile load, then the initiated crack will easily propagate and move though weak area of the cell wall and meet another defected area as represented by red lines, in this manner crack is initiated and propagated and sample become failed.

**Figure 11.** Stress vs. strain curves of tensile test for 20 pores per inch specimens

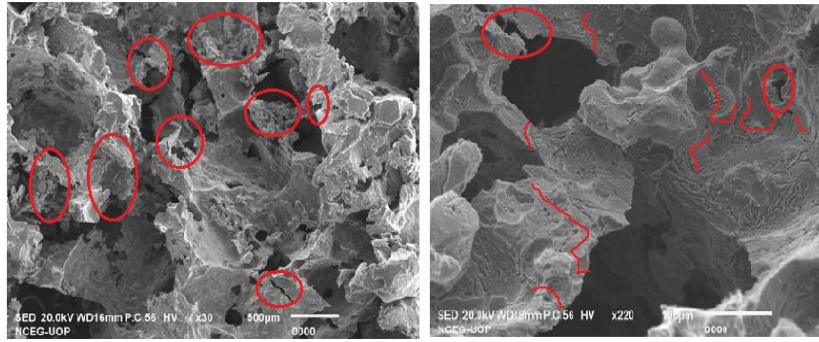


Figure 12. SEM micrograph of fracture surface of 20 pores per inch after tensile test

Table 2. Tensile properties of 20 ppi of open cell aluminum foam by Alporas rout

Samples	Dimensions (LxBxW) (mm)	Young's Modulus (MPa)	Stress at yield (MPa)	UTS (MPa)	Elongation at yield (mm)	Elongation at break (mm)
20-A	71x15x8	691.54	0.725	7.52	0.078	1.386
20-B	71x15x8	1265.9	3.273	18	0.44	1.16
20-C	71x15x8	795.76	0.767	6.68	0.346	1.601
Average	-	743.65	1.588	7.1	0.288	1.392

The Young's Modulus of 1036.1 MPa and UTS of 18 MPa of 20-B is outlier which is not consider in average value.

### Compression Test

Energy absorption being the most important applications of metal foam required the need of characterizing 20 ppi for their mechanical properties on the basis of pore size per unit length. Figure 13 shows stress versus strain curves of 20 ppi under compression test of the three samples of the same pores. The details parameters and properties of each tested sample were summarized in Table 3. The young modulus of 20-C shows far-off behaviour and consider as outlier. Because its young modulus is 1036.1 MPa which is very higher as compared with other two samples of the same pores. However other properties of the three specimens of 20 ppi are nearly same so their corresponding average is calculated. Based on average value, it can be seen that 62.49% of maximum strain were obtained at peak stress of 107.26 MPa. The two main properties of interest in the compression test are plateau stress and energy absorption at a given strain. The average plateau stress is 28.53 MPa and energy absorption is 376.45 N-m were noticed after compression test. Plateau stresses were calculated according to standard ISO 13314:2011. Arithmetic mean of stresses at 20% strain and 40% were taken to give us the plateau stress. This stress indicates the value of stress required for complete collapse of pores in metal foam. After foam is collapsed, densification sets to starts which also act as compaction. Densification is important to find out because it gives the quality of energy absorption of that foam. Literature suggests that densification strain between 50-55% strain is ideal. Figure 14 shows the microstructure of fractured surface of the samples after the compression test experiment. It was identified that all pores are collapsed and the boundary of collapsed cells represented by red lines. The pores/cells collapsing occurred in plateau region of the stress-strain graph, where the plateau region is considered the area in between 20% and 40% strain of the graph. When all pores are collapsed, densification sets to starts which also act as compaction. During densification process numbers of cracks and crumples on the cell wall appeared which caused by the brittleness of the cell wall as shown in red circle and orange color box. When compactions of the pores are completed, a major failure like flake-off on the outer surface of the sample will appeared.

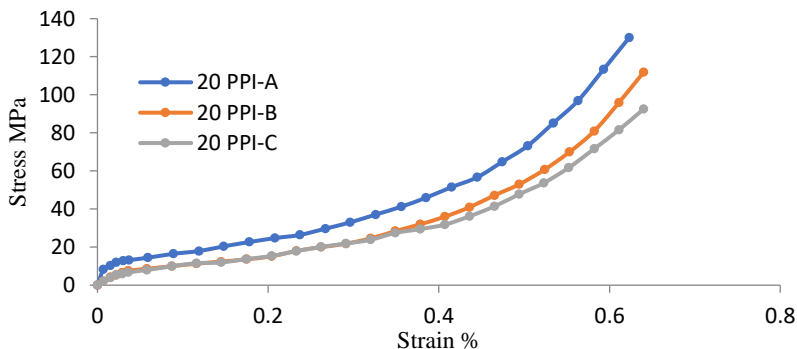


Figure 13. Stress vs. strain curves of compression test for 20 pores per inch specimens

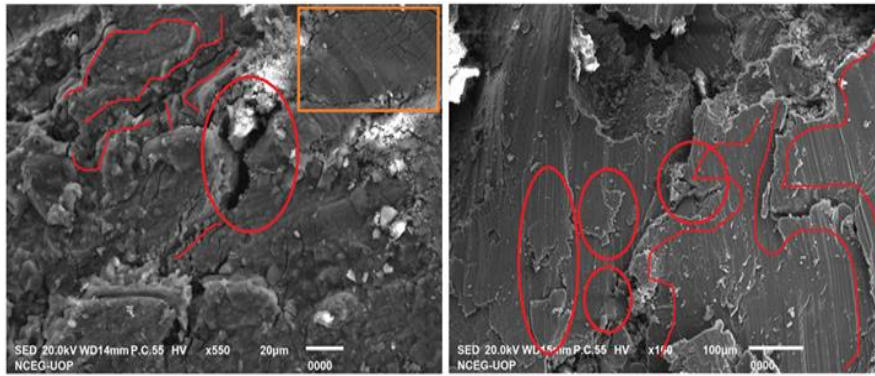


Figure 14. SEM micrograph of fracture surface of 20 pores per inch after compression test

Table 3. Compression properties of 20 ppi of open cell aluminum foam by Alporas rout

Samples	Dimensions (LxHxW) (mm)	Young's Modulus (MPa)	Stress at yield (MPa)	Stress at Peak (MPa)	Plateau Stress (MPa)	Densification strain/ Plateau end strain (%)	Energy absorption at Peak Stress (NM)	Peak strain (%)
20-A	34x34x15	88.763	26.053	129.98	36	39.8	450.41	62.37
20-B	34x34x15	86.26	19.912	99.2	26.1	39.4	345.72	62.152
20-C	34x34x15	1036.1	18.536	92.6	23.5	38.7	333.22	62.96
Average	-	87.51	21.500	107.26	28.53	39.3	376.45	62.49

The Young's Modulus of 1036.1 MPa is outlier which is not consider in average value

Hardness Test

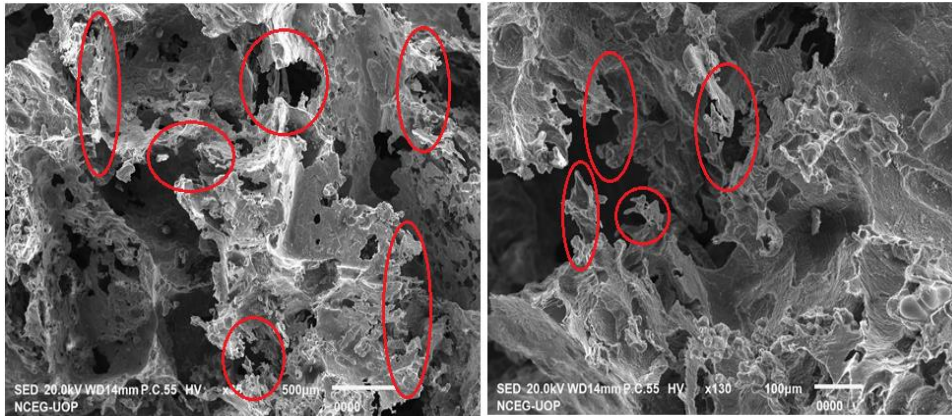
The Table 4 presented the hardness values of open cell aluminium foam with 20 ppi of Alporas rout in four trials and their average value is 3.65 HRV1. It can be noticed that the obtained hardness valves is actually the hardness of the solid state of the aluminium foam. The hardness could be further increased by decreasing number of pores per unit length. The main reason behind this is to reduce the number of pores per unit length will lead to increase the volume percentage of solid state and the hardness of the solid fraction/contents is significantly higher than the cell wall.

Table 4. Hardness values of 20 ppi of open cell aluminum foam by Alporas rout

Scale: HV1	Dwell Time: 10 Sec				Load: 1 kgf	
Sample I.D	Test 1	Test 2	Test 3	Test 4	Average	S. Deviation
20 PPI	2.74	3.25	5.1	3.5	3.6475	1.02

Charpy Impact Test

The Table 5 displayed the energy engrossed by the specimens of 20 ppi of Alporas rout in four times and their average value is 366.3 J/m<sup>2</sup>. This quantitative result of dynamic loading can be calculated from the energy needed to fracture a specimens and can be used to measure the toughness of the aluminium foam. The qualitative result of dynamic loading can be used to determine the ductility of material. If the material breaks on a flat plane, the fracture was brittle, and if the material breaks with jagged edges or shear lips, then the fracture was ductile. Usually open cell aluminum foam of alporas does not break in just one way or the other, and thus comparing the jagged to flat surface areas of the fracture will give idea of ductile and brittle fracture. It also shows importance for applications that require lightweight structures with a high capacity of energy dissipation, such as the transport industry, where problems of collision and crash have increased. Figure 15 expresses the microstructure of fractured surface of specimens after the charpy impact test. The shredded cell walls with shear lips of the two adjoining cell were looked-over which is looking like ductile in nature as represented by red circle. Some micro cracks were found on the surface of the cell walls and these cracks propagate and move though the week area of the cells and join one another as a result of which macro crack are created and material failed.



**Figure 15.** SEM micrograph of fracture surface of 20 pores per inch after Charpy impact test

**Table 5.** Energy absorption of 20 ppi of open cell aluminum foam by Alporas rout under impact

Sample	Test-1 (J/m <sup>2</sup> )	Test-1 (J/m <sup>2</sup> )	Test-1 (J/m <sup>2</sup> )	Test-1 (J/m <sup>2</sup> )	Average	S. Deviation
20 PPI	338	338	376	413	366.3	36

## CONCLUSION

In this study, three point bending test, vickers hardness test, tensile test, compression test and Charpy impact test have been performed on open cell aluminum foam with 20 pores per inch (ppi) prepared by Alporas rout. The following findings are condensed.

In bending test, failure occurred in three steps: (i) elastic deformation region (ii) creation and appearance of micro cracks (iii) failure stage; and macro cracks appeared at the center of the specimens on tension side. The average bending strength 4.69 MPa were observed at the peak force. In stress-strain curve of the tensile test, after reaching elastic limit a flat behavior curve similar to plastic deformation flow were noticed where strain is continuously increases at constant stress and then reached to peak stress and 7.1 MPa is average ultimate strength was noticed. The two important properties in the compression test; plateau stress and energy absorption at a given strain were observed. The average plateau stress is 28.53 MPa and energy absorption is 376.45 N-m were noticed and failure was occurred in three stages (I-elastic, II-plateau and II-densification) and all cell are collapsed in second stage. The bending strength, tensile strength and compression properties could be increased if number of pores per unit length increased. The average hardness value is 3.65 HRV1 were obtained. It can be observed that the obtained hardness value is actually the hardness of the solid state/phase of the aluminium foam. In sudden impact, the average energy absorption is 519 J/m<sup>2</sup> was noticed. The hardness and sudden impact properties could also be increased if number of pores per unit length decreased. From SEM images, the shredded cell wall is looked over which was ductile in nature and have occurred in flexural, tensile and Charpy impact load tested specimens. All pores are collapsed in plateau region, and some crumples and brittle tiny cracks are detected in densifications stage. Moreover some patterned grooves but not deeper, were noticed on the surface of the cell wall which may also take active part in the creations of micro cracks during loading.

## ACKNOWLEDGEMENT

This work is approved and supported by University of Engineering and Technology Peshawar, Pakistan.

## REFERENCES

- [1] C. Motz and R. Pippin, "Deformation behaviour of closed-cell aluminium foams in tension," *Acta Materialia*, vol. 49, no. 13, pp. 2463-2470, 2001, doi: 10.1016/S1359-6454(01)00152-5.
- [2] J. Liu, S. He, H. Zhao, G. Li, and M. Wang, "Experimental investigation on the dynamic behaviour of metal foam: From yield to densification," *International Journal of Impact Engineering*, vol. 114, pp. 69-77, 2018, doi: 10.1016/j.ijimpeng.2017.12.016.
- [3] J. Banhart, "Manufacture, characterisation and application of cellular metals and metal foams," *Progress in Materials Science*, vol. 46, no. 6, pp. 559-632, 2001, doi: 10.1016/S0079-6425(00)00002-5.
- [4] G. Castro and S. R. Nutt, "Synthesis of syntactic steel foam using mechanical pressure infiltration," *Materials Science and Engineering: A*, vol. 535, pp. 274-280, 2012, doi: 10.1016/j.msea.2011.12.084.
- [5] A. G. Evans, J. W. Hutchinson, and M. F. Ashby, "Multifunctionality of cellular metal systems," *Progress in Materials Science*, vol. 43, no. 3, pp. 171-221, 1998, doi: 10.1016/S0079-6425(98)00004-8.

- [6] J. Baumeister, J. Banhart, and M. Weber, "Aluminium foams for transport industry," *Materials & Design*, vol. 18, no. 4, pp. 217-220, 1997, doi: 10.1016/S0261-3069(97)00050-2.
- [7] Z. Xu and H. Hao, "Electromagnetic interference shielding effectiveness of aluminum foams with different porosity," *Journal of Alloys and Compounds*, vol. 617, pp. 207-213, 2014, doi: 10.1016/j.jallcom.2014.07.188.
- [8] B. Hamidi Ghaleh Jigh, H. Hosseini-Toudeshky, and M. A. Farsi, "Low cycle fatigue analyses of open-celled aluminum foam under compression-compression loading using experimental and microstructure finite element analysis," *Journal of Alloys and Compounds*, vol. 797, pp. 231-236, 2019, doi: 10.1016/j.jallcom.2019.05.158.
- [9] Y. Wang, X. Zhai, and W. Wang, "Numerical studies of aluminum foam filled energy absorption connectors under quasi-static compression loading," *Thin-Walled Structures*, vol. 116, pp. 225-233, 2017, doi: 10.1016/j.tws.2017.03.032.
- [10] M. Saadatfar *et al.*, "Structure and deformation correlation of closed-cell aluminium foam subject to uniaxial compression," *Acta Materialia*, vol. 60, no. 8, pp. 3604-3615, 2012, doi: 10.1016/j.actamat.2012.02.029.
- [11] M. Taherishargh, E. Linul, S. Broxtermann, and T. Fiedler, "The mechanical properties of expanded perlite-aluminium syntactic foam at elevated temperatures," *Journal of Alloys and Compounds*, vol. 737, pp. 590-596, 2018, doi: 10.1016/j.jallcom.2017.12.083.
- [12] E. Linul, N. Movahedi, and L. Marsavina, "The temperature and anisotropy effect on compressive behavior of cylindrical closed-cell aluminum-alloy foams," *Journal of Alloys and Compounds*, vol. 740, pp. 1172-1179, 2018, doi: 10.1016/j.jallcom.2018.01.102.
- [13] M. A. Islam *et al.*, "Mechanical response and dynamic deformation mechanisms of closed-cell aluminium alloy foams under dynamic loading," *International Journal of Impact Engineering*, vol. 114, pp. 111-122, 2018, doi: 10.1016/j.ijimpeng.2017.12.012.
- [14] X. Pang and H. Du, "Dynamic characteristics of aluminium foams under impact crushing," *Composites Part B: Engineering*, vol. 112, pp. 265-277, 2017, doi: 10.1016/j.compositesb.2016.12.044.
- [15] Y. Zhang, Q. Liu, Z. He, Z. Zong, and J. Fang, "Dynamic impact response of aluminum honeycombs filled with Expanded Polypropylene foam," *Composites Part B: Engineering*, vol. 156, pp. 17-27, 2019, doi: 10.1016/j.compositesb.2018.08.043.
- [16] R. P. Merrett, G. S. Langdon, and M. D. Theobald, "The blast and impact loading of aluminium foam," *Materials & Design*, vol. 44, pp. 311-319, 2013, doi: <https://doi.org/10.1016/j.matdes.2012.08.016>.
- [17] V. C. Shunmugasamy and B. Mansoor, "Compressive behavior of a rolled open-cell aluminum foam," *Materials Science and Engineering: A*, vol. 715, pp. 281-294, 2018, doi: 10.1016/j.msea.2018.01.015.
- [18] Y. K. An, S. Y. Yang, E. T. Zhao, and H. A. Zhou, "Formation mechanism and three-point bending behaviour of directly fabricated aluminium foam plates," *Materials Science and Technology*, vol. 33, no. 4, pp. 421-429, 2017, doi: 10.1080/02670836.2016.1221494.
- [19] M. Sangeetha, S. Prakash, K. S. Sridharraja, and J. Muralimano, "Development, testing and microstructural study of aluminum foam in automobile application," *International Journal of Ambient Energy*, vol. 43, no. 1, pp. 2568-2576, 2022, doi: 10.1080/01430750.2020.1723690.
- [20] X. Yang *et al.*, "Compression fatigue properties of open-cell aluminum foams fabricated by space-holder method," *International Journal of Fatigue*, vol. 121, pp. 272-280, 2019, doi: 10.1016/j.ijfatigue.2018.11.008.
- [21] H. Yu, G. Yao, X. Wang, Y. Liu, and H. Li, "Sound insulation property of Al-Si closed-cell aluminum foam sandwich panels," *Applied Acoustics*, vol. 68, no. 11, pp. 1502-1510, 2007, doi: 10.1016/j.apacoust.2006.07.019.
- [22] R. E. Raj and B. S. S. Daniel, "Aluminum melt foam processing for light-weight structures," *Materials and Manufacturing Processes*, vol. 22, no. 4, pp. 525-530, 2007, doi: 10.1080/10426910701236072.
- [23] R. Soltani, Z. Sarajan, and M. Soltani, "Foaming of pure aluminium by TiH<sub>2</sub>," *Materials Research Innovations*, vol. 18, no. 6, pp. 401-406, 2014, doi: 10.1179/1433075X13Y.0000000161.
- [24] M. Ulbin *et al.*, "Low cycle fatigue behaviour of closed-cell aluminium foam," *Mechanics of Materials*, vol. 133, pp. 165-173, 2019, doi: 10.1016/j.mechmat.2019.03.014.